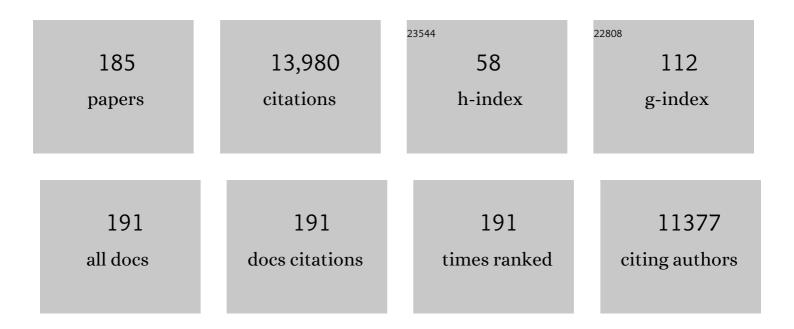
## Min Zhu

## List of Publications by Year in descending order

Source: https://exaly.com/author-pdf/8754/publications.pdf Version: 2024-02-01



Мім 7нц

#	Article	IF	CITATIONS
1	Zn/MnO <sub>2</sub> Battery Chemistry With H <sup>+</sup> and Zn <sup>2+</sup> Coinsertion. Journal of the American Chemical Society, 2017, 139, 9775-9778.	6.6	1,375
2	Ammonia Electrosynthesis with High Selectivity under Ambient Conditions via a Li <sup>+</sup> Incorporation Strategy. Journal of the American Chemical Society, 2017, 139, 9771-9774.	6.6	547
3	Recent advances and remaining challenges of nanostructured materials for hydrogen storage applications. Progress in Materials Science, 2017, 88, 1-48.	16.0	526
4	New Nanoconfined Galvanic Replacement Synthesis of Hollow Sb@C Yolk–Shell Spheres Constituting a Stable Anode for High-Rate Li/Na-Ion Batteries. Nano Letters, 2017, 17, 2034-2042.	4.5	386
5	A Ceneral Metalâ€Organic Framework (MOF)â€Derived Selenidation Strategy for In Situ Carbonâ€Encapsulated Metal Selenides as Highâ€Rate Anodes for Naâ€Ion Batteries. Advanced Functional Materials, 2018, 28, 1707573.	7.8	325
6	Stabilizing the Nanostructure of SnO <sub>2</sub> Anodes by Transition Metals: A Route to Achieve High Initial Coulombic Efficiency and Stable Capacities for Lithium Storage. Advanced Materials, 2017, 29, 1605006.	11.1	306
7	Enhancing the Regeneration Process of Consumed NaBH <sub>4</sub> for Hydrogen Storage. Advanced Energy Materials, 2017, 7, 1700299.	10.2	304
8	Application of dielectric barrier discharge plasma-assisted milling in energy storage materials – A review. Journal of Alloys and Compounds, 2017, 691, 422-435.	2.8	301
9	Dramatically enhanced reversibility of Li <sub>2</sub> 0 in SnO <sub>2</sub> -based electrodes: the effect of nanostructure on high initial reversible capacity. Energy and Environmental Science, 2016, 9, 595-603.	15.6	300
10	Monodisperse Magnesium Hydride Nanoparticles Uniformly Selfâ€Assembled on Graphene. Advanced Materials, 2015, 27, 5981-5988.	11.1	298
11	Mg–TM (TM: Ti, Nb, V, Co, Mo or Ni) core–shell like nanostructures: synthesis, hydrogen storage performance and catalytic mechanism. Journal of Materials Chemistry A, 2014, 2, 9645-9655.	5.2	248
12	Robust Pitaya-Structured Pyrite as High Energy Density Cathode for High-Rate Lithium Batteries. ACS Nano, 2017, 11, 9033-9040.	7.3	247
13	Remarkable enhancement in dehydrogenation of MgH2 by a nano-coating of multi-valence Ti-based catalysts. Journal of Materials Chemistry A, 2013, 1, 5603.	5.2	221
14	Self‣upported and Flexible Sulfur Cathode Enabled via Synergistic Confinement for Highâ€Energyâ€Density Lithium–Sulfur Batteries. Advanced Materials, 2019, 31, e1902228.	11.1	216
15	Mechanistic Understanding of Metal Phosphide Host for Sulfur Cathode in High-Energy-Density Lithium–Sulfur Batteries. ACS Nano, 2019, 13, 8986-8996.	7.3	215
16	Closing the Loop for Hydrogen Storage: Facile Regeneration of NaBH <sub>4</sub> from its Hydrolytic Product. Angewandte Chemie - International Edition, 2020, 59, 8623-8629.	7.2	205
17	Advances in the Development of Singleâ€Atom Catalysts for Highâ€Energyâ€Density Lithium–Sulfur Batteries. Advanced Materials, 2022, 34, e2200102.	11.1	202
18	Electrospun Thin-Walled CuCo <sub>2</sub> O <sub>4</sub> @C Nanotubes as Bifunctional Oxygen Electrocatalysts for Rechargeable Zn–Air Batteries. Nano Letters, 2017, 17, 7989-7994.	4.5	199

#	Article	IF	CITATIONS
19	Uniform Hierarchical Fe <sub>3</sub> O <sub>4</sub> @Polypyrrole Nanocages for Superior Lithium Ion Battery Anodes. Advanced Energy Materials, 2016, 6, 1600256.	10.2	184
20	Regulating Lithium Nucleation and Deposition via MOFâ€Derived Co@Câ€Modified Carbon Cloth for Stable Li Metal Anode. Advanced Functional Materials, 2020, 30, 1909159.	7.8	170
21	Symbiotic CeH 2.73 /CeO 2 catalyst: A novel hydrogen pump. Nano Energy, 2014, 9, 80-87.	8.2	159
22	Thermodynamic Tuning of Mg-Based Hydrogen Storage Alloys: A Review. Materials, 2013, 6, 4654-4674.	1.3	157
23	Inhibiting grain coarsening and inducing oxygen vacancies: the roles of Mn in achieving a highly reversible conversion reaction and a long life SnO <sub>2</sub> –Mn–graphite ternary anode. Energy and Environmental Science, 2017, 10, 2017-2029.	15.6	152
24	Converting H <sup>+</sup> from coordinated water into H <sup>â^'</sup> enables super facile synthesis of LiBH <sub>4</sub> . Green Chemistry, 2019, 21, 4380-4387.	4.6	149
25	Mesoporous Mo <sub>2</sub> C/N-doped carbon heteronanowires as high-rate and long-life anode materials for Li-ion batteries. Journal of Materials Chemistry A, 2016, 4, 10842-10849.	5.2	143
26	A Novel Strategy to Suppress Capacity and Voltage Fading of Li―and Mnâ€Rich Layered Oxide Cathode Material for Lithiumâ€Ion Batteries. Advanced Energy Materials, 2017, 7, 1601066.	10.2	141
27	A mechanical-force-driven physical vapour deposition approach to fabricating complex hydride nanostructures. Nature Communications, 2014, 5, 3519.	5.8	136
28	Sandwich-like SnS/Polypyrrole Ultrathin Nanosheets as High-Performance Anode Materials for Li-Ion Batteries. ACS Applied Materials & Interfaces, 2016, 8, 8502-8510.	4.0	133
29	Silicon/graphene based nanocomposite anode: large-scale production and stable high capacity for lithium ion batteries. Journal of Materials Chemistry A, 2014, 2, 9118-9125.	5.2	131
30	Metal–Organic Framework-Derived NiSb Alloy Embedded in Carbon Hollow Spheres as Superior Lithium-Ion Battery Anodes. ACS Applied Materials & Interfaces, 2017, 9, 2516-2525.	4.0	116
31	Embedding nano-silicon in graphene nanosheets by plasma assisted milling for high capacity anode materials in lithium ion batteries. Journal of Power Sources, 2014, 268, 610-618.	4.0	110
32	llmenite Nanotubes for High Stability and High Rate Sodium-Ion Battery Anodes. ACS Nano, 2017, 11, 5120-5129.	7.3	109
33	Hydrogen generation via hydrolysis of magnesium with seawater using Mo, MoO <sub>2</sub> , MoO <sub>3</sub> and MoS <sub>2</sub> as catalysts. Journal of Materials Chemistry A, 2017, 5, 8566-8575.	5.2	103
34	Sn@SnOx/C nanocomposites prepared by oxygen plasma-assisted milling as cyclic durable anodes for lithium ion batteries. Journal of Power Sources, 2013, 242, 114-121.	4.0	94
35	FeP@C Nanotube Arrays Grown on Carbon Fabric as a Low Potential and Freestanding Anode for Highâ€Performance Liâ€Ion Batteries. Small, 2018, 14, e1800793.	5.2	94
36	Hierarchical MoO <sub>2</sub> /Mo <sub>2</sub> C/C Hybrid Nanowires as High-Rate and Long-Life Anodes for Lithium-Ion Batteries. ACS Applied Materials & Interfaces, 2016, 8, 19987-19993.	4.0	92

#	Article	IF	CITATIONS
37	Enhanced Hydrogen Generation Properties of MgH2-Based Hydrides by Breaking the Magnesium Hydroxide Passivation Layer. Energies, 2015, 8, 4237-4252.	1.6	90
38	Express penetration of hydrogen on Mg(10ĺž13) along the close-packed-planes. Scientific Reports, 2015, 5, 10776.	1.6	89
39	A long-life nano-silicon anode for lithium ion batteries: supporting of graphene nanosheets exfoliated from expanded graphite by plasma-assisted milling. Electrochimica Acta, 2016, 187, 1-10.	2.6	89
40	Unraveling the Catalytic Activity of Fe–Based Compounds toward Li <sub>2</sub> S <i><sub>x</sub></i> in Li–S Chemical System from <i>d</i> – <i>p</i> Bands. Advanced Energy Materials, 2021, 11, 2100673.	10.2	89
41	A new method for few-layer graphene preparation via plasma-assisted ball milling. Journal of Alloys and Compounds, 2017, 728, 578-584.	2.8	86
42	Phase Stability, Structural Transition, and Hydrogen Absorptionâ^'Desorption Features of the Polymorphic La <sub>4</sub> MgNi <sub>19</sub> Compound. Journal of Physical Chemistry C, 2010, 114, 11686-11692.	1.5	83
43	Sn–C and Se–C Co-Bonding SnSe/Few-Layered Graphene Micro–Nano Structure: Route to a Densely Compacted and Durable Anode for Lithium/Sodium-Ion Batteries. ACS Applied Materials & Interfaces, 2019, 11, 36685-36696.	4.0	83
44	Unveiling the Advances of Nanostructure Design for Alloyâ€Type Potassiumâ€Ion Battery Anodes via Inâ€Situ TEM. Angewandte Chemie - International Edition, 2020, 59, 14504-14510.	7.2	82
45	Constructing Liâ€Rich Artificial SEI Layer in Alloy–Polymer Composite Electrolyte to Achieve High Ionic Conductivity for Allâ€Solidâ€State Lithium Metal Batteries. Advanced Materials, 2021, 33, e2004711.	11.1	82
46	Unveiling critical size of coarsened Sn nanograins for achieving high round-trip efficiency of reversible conversion reaction in lithiated SnO2 nanocrystals. Nano Energy, 2018, 45, 255-265.	8.2	80
47	In Situ Construction a Stable Protective Layer in Polymer Electrolyte for Ultralong Lifespan Solidâ€State Lithium Metal Batteries. Advanced Science, 2022, 9, e2104277.	5.6	78
48	A flexible composite solid electrolyte with a highly stable interphase for dendrite-free and durable all-solid-state lithium metal batteries. Journal of Materials Chemistry A, 2020, 8, 18043-18054.	5.2	77
49	A Self-Supporting Covalent Organic Framework Separator with Desolvation Effect for High Energy Density Lithium Metal Batteries. ACS Energy Letters, 2022, 7, 885-896.	8.8	76
50	Selfâ€5upported CoP Nanorod Arrays Grafted on Stainless Steel as an Advanced Integrated Anode for Stable and Longâ€Life Lithiumâ€lon Batteries. Chemistry - A European Journal, 2017, 23, 5198-5204.	1.7	75
51	Facile synthesis of Ge@FLG composites by plasma assisted ball milling for lithium ion battery anodes. Journal of Materials Chemistry A, 2014, 2, 11280-11285.	5.2	74
52	A highly stable (SnO x -Sn)@few layered graphene composite anode of sodium-ion batteries synthesized by oxygen plasma assisted milling. Journal of Power Sources, 2017, 350, 1-8.	4.0	74
53	A scalable ternary SnO <sub>2</sub> –Co–C composite as a high initial coulombic efficiency, large capacity and long lifetime anode for lithium ion batteries. Journal of Materials Chemistry A, 2018, 6, 7206-7220.	5.2	74
54	Tinâ€Based Anode Materials for Stable Sodium Storage: Progress and Perspective. Advanced Materials, 2022, 34, e2106895.	11.1	68

#	Article	IF	CITATIONS
55	Interface engineering for composite cathodes in sulfide-based all-solid-state lithium batteries. Journal of Energy Chemistry, 2021, 60, 32-60.	7.1	64
56	A spherical Sn–Fe <sub>3</sub> O <sub>4</sub> @graphite composite as a long-life and high-rate-capability anode for lithium ion batteries. Journal of Materials Chemistry A, 2016, 4, 10321-10328.	5.2	63
57	Robust spindle-structured FeP@C for high-performance alkali-ion batteries anode. Electrochimica Acta, 2019, 312, 224-233.	2.6	62
58	Hydrogen Production via Hydrolysis and Alcoholysis of Light Metal-Based Materials: A Review. Nano-Micro Letters, 2021, 13, 134.	14.4	62
59	High-performance anode materials for Na-ion batteries. Rare Metals, 2018, 37, 167-180.	3.6	60
60	Lithium Difluorophosphate As a Promising Electrolyte Lithium Additive for High-Voltage Lithium-Ion Batteries. ACS Applied Energy Materials, 2018, 1, 2647-2656.	2.5	60
61	Biomedical Porous Shape Memory Alloys for Hard-Tissue Replacement Materials. Materials, 2018, 11, 1716.	1.3	59
62	Ultralow Volume Change of P2â€Type Layered Oxide Cathode for Naâ€Ion Batteries with Controlled Phase Transition by Regulating Distribution of Na <sup>+</sup> . Angewandte Chemie - International Edition, 2021, 60, 20960-20969.	7.2	59
63	A nanorod-like Ni-rich layered cathode with enhanced Li <sup>+</sup> diffusion pathways for high-performance lithium-ion batteries. Journal of Materials Chemistry A, 2021, 9, 2830-2839.	5.2	58
64	Novel nitrogen-rich porous carbon spheres as a high-performance anode material for lithium-ion batteries. Journal of Materials Chemistry A, 2014, 2, 16617-16622.	5.2	57
65	Hierarchical nanoflowers assembled from MoS 2 /polyaniline sandwiched nanosheets for high-performance supercapacitors. Electrochimica Acta, 2017, 243, 98-104.	2.6	56
66	Self-sacrificial template-directed ZnSe@C as high performance anode for potassium-ion batteries. Chemical Engineering Journal, 2020, 387, 124061.	6.6	55
67	Inhibiting Sn coarsening to enhance the reversibility of conversion reaction in lithiated SnO2 anodes by application of super-elastic NiTi films. Acta Materialia, 2016, 109, 248-258.	3.8	54
68	Sn buffered by shape memory effect of NiTi alloys as high-performance anodes for lithium ion batteries. Acta Materialia, 2012, 60, 4695-4703.	3.8	53
69	Progress on Sn-based thin-film anode materials for lithium-ion batteries. Science Bulletin, 2012, 57, 4119-4130.	1.7	53
70	Fully Reversible De/hydriding of Mg Base Solid Solutions with Reduced Reaction Enthalpy and Enhanced Kinetics. Journal of Physical Chemistry C, 2014, 118, 12087-12096.	1.5	53
71	Highly Stable Cycling of Amorphous Li <sub>2</sub> CO <sub>3</sub> -Coated α-Fe <sub>2</sub> O <sub>3</sub> Nanocrystallines Prepared via a New Mechanochemical Strategy for Li-Ion Batteries. Advanced Functional Materials, 2017, 27, 1605011.	7.8	53
72	Co-Substitution Enhances the Rate Capability and Stabilizes the Cyclic Performance of O3-Type Cathode NaNi <sub>0.45–<i>x</i></sub> Mn <sub>0.25</sub> Ti <sub>0.3</sub> Co <sub><i>x</i></sub> O <sub>2</sub> for Sodium-Ion Storage at High Voltage. ACS Applied Materials & Interfaces, 2019, 11, 7906-7913.	· 4.0	53

#	Article	IF	CITATIONS
73	Towards easy reversible dehydrogenation of LiBH 4 by catalyzing hierarchic nanostructured CoB. Nano Energy, 2014, 10, 235-244.	8.2	52
74	Enhanced hydrogen storage properties of a Mg–Ag alloy with solid dissolution of indium: a comparative study. Journal of Materials Chemistry A, 2015, 3, 8581-8589.	5.2	52
75	B,N Codoped Graphitic Nanotubes Loaded with Co Nanoparticles as Superior Sulfur Host for Advanced Li–S Batteries. Small, 2020, 16, e1906634.	5.2	50
76	N-doped carbon encapsulated CoMoO4 nanorods as long-cycle life anode for sodium-ion batteries. Journal of Colloid and Interface Science, 2020, 576, 176-185.	5.0	50
77	Microstructure and electrochemical performance of thin film anodes for lithium ion batteries in immiscible Al–Sn system. Journal of Power Sources, 2009, 188, 268-273.	4.0	49
78	A New Strategy to Effectively Suppress the Initial Capacity Fading of Iron Oxides by Reacting with LiBH <sub>4</sub> . Advanced Functional Materials, 2017, 27, 1700342.	7.8	49
79	A Recycling Hydrogen Supply System of NaBH4 Based on a Facile Regeneration Process: A Review. Inorganics, 2018, 6, 10.	1.2	48
80	Unveiling the Advances of Nanostructure Design for Alloyâ€Type Potassiumâ€Ion Battery Anodes via Inâ€Situ TEM. Angewandte Chemie, 2020, 132, 14612-14618.	1.6	47
81	Synergetic effects of hydrogenated Mg3La and TiCl3 on the dehydrogenation of LiBH4. Journal of Materials Chemistry, 2011, 21, 9179.	6.7	46
82	Deformable fibrous carbon supported ultrafine nano-SnO <sub>2</sub> as a high volumetric capacity and cyclic durable anode for Li storage. Journal of Materials Chemistry A, 2015, 3, 15097-15107.	5.2	46
83	Solvent-Free Method Prepared a Sandwich-like Nanofibrous Membrane-Reinforced Polymer Electrolyte for High-Performance All-Solid-State Lithium Batteries. ACS Applied Materials & Interfaces, 2020, 12, 21586-21595.	4.0	46
84	Enhancing the performance of Sn–C nanocomposite as lithium ion anode by discharge plasma assisted milling. Journal of Materials Chemistry, 2012, 22, 8022.	6.7	44
85	Confined LiBH4: Enabling fast hydrogen release at â^¼100°C. International Journal of Hydrogen Energy, 2012, 37, 18920-18926.	3.8	44
86	3,3′-(Ethylenedioxy)dipropiononitrile as an Electrolyte Additive for 4.5 V LiNi <sub>1/3</sub> Co <sub>1/3</sub> Mn <sub>1/3</sub> O <sub>2</sub> /Graphite Cells. ACS Applied Materials & Interfaces, 2017, 9, 9630-9639.	4.0	43
87	Origin of Capacity Increasing in a Longâ€Life Ternary Sn–Fe <sub>3</sub> O <sub>4</sub> @Graphite Anode for Liâ€lon Batteries. Advanced Materials Interfaces, 2017, 4, 1700113.	1.9	43
88	Facile synthesis of self-supported Mn <sub>3</sub> O <sub>4</sub> @C nanotube arrays constituting an ultrastable and high-rate anode for flexible Li-ion batteries. Journal of Materials Chemistry A, 2017, 5, 8555-8565.	5.2	41
89	Mesoporous Fe <sub>2</sub> O <sub>3</sub> flakes of high aspect ratio encased within thin carbon skeleton for superior lithium-ion battery anodes. Journal of Materials Chemistry A, 2015, 3, 14178-14187.	5.2	40
90	AlH3 as a hydrogen storage material: recent advances, prospects and challenges. Rare Metals, 2021, 40, 3337-3356.	3.6	40

#	Article	IF	CITATIONS
91	Insight into Reversible Conversion Reactions in SnO <sub>2</sub> â€Based Anodes for Lithium Storage: A Review. Small, 2022, 18, e2201110.	5.2	40
92	Enhanced high-voltage cyclability of LiNi0.5Co0.2Mn0.3O2-based pouch cells via lithium difluorophosphate introducing as electrolyte additive. Journal of Alloys and Compounds, 2018, 755, 1-9.	2.8	39
93	Realizing facile regeneration of spent NaBH <sub>4</sub> with Mg–Al alloy. Journal of Materials Chemistry A, 2019, 7, 10723-10728.	5.2	39
94	Closing the Loop for Hydrogen Storage: Facile Regeneration of NaBH <sub>4</sub> from its Hydrolytic Product. Angewandte Chemie, 2020, 132, 8701-8707.	1.6	39
95	General construction of lithiophilic 3D skeleton for dendrite-free lithium metal anode via a versatile MOF-derived route. Science China Materials, 2022, 65, 337-348.	3.5	38
96	An amorphous wrapped nanorod LiV3O8 electrode with enhanced performance for lithium ion batteries. RSC Advances, 2012, 2, 7273.	1.7	37
97	Core/shell and multi-scale structures enhance the anode performance of a Sn–C–Ni composite thin film in a lithium ion battery. Journal of Materials Chemistry, 2011, 21, 4629.	6.7	36
98	A novel selenium-phosphorous amorphous composite by plasma assisted ball milling for high-performance rechargeable potassium-ion battery anode. Journal of Power Sources, 2019, 443, 227276.	4.0	36
99	Thermal stability, decomposition and glass transition behavior of PANI/NiO composites. Journal of Thermal Analysis and Calorimetry, 2009, 98, 533-537.	2.0	35
100	Metals (Ni, Fe)-Incorporated Titanate Nanotubes Induced Destabilization of LiBH <sub>4</sub> . Journal of Physical Chemistry C, 2011, 115, 9780-9786.	1.5	35
101	A novel method for the synthesis of solvent-free Mg(B <sub>3</sub> H <sub>8</sub> ) <sub>2</sub> . Dalton Transactions, 2016, 45, 3687-3690.	1.6	35
102	Synthesis of N-doped hierarchical carbon spheres for CO <sub>2</sub> capture and supercapacitors. RSC Advances, 2016, 6, 1422-1427.	1.7	35
103	3D Hierarchical Porous Cu-Based Composite Current Collector with Enhanced Ligaments for Notably Improved Cycle Stability of Sn Anode in Li-Ion Batteries. ACS Applied Materials & Interfaces, 2018, 10, 22050-22058.	4.0	35
104	Nanoconfined Oxidation Synthesis of Nâ€Doped Carbon Hollow Spheres and MnO <sub>2</sub> Encapsulated Sulfur Cathode for Superior Liâ€5 Batteries. Chemistry - A European Journal, 2018, 24, 4573-4582.	1.7	34
105	<i>In Situ</i> Embedding of Mg <sub>2</sub> NiH <sub>4</sub> and YH <sub>3</sub> Nanoparticles into Bimetallic Hydride NaMgH <sub>3</sub> to Inhibit Phase Segregation for Enhanced Hydrogen Storage. Journal of Physical Chemistry C, 2014, 118, 23635-23644.	1.5	33
106	Engineering layer structure of MoS2/polyaniline/graphene nanocomposites to achieve fast and reversible lithium storage for high energy density aqueous lithium-ion capacitors. Journal of Power Sources, 2020, 450, 227680.	4.0	33
107	Silicon/Wolfram Carbide@Graphene composite: enhancing conductivity and structure stability in amorphous-silicon for high lithium storage performance. Electrochimica Acta, 2016, 191, 462-472.	2.6	32
108	Synthesis and hydrolysis of NaZn(BH4)3 and its ammoniates. Journal of Materials Chemistry A, 2017, 5, 17012-17020.	5.2	32

#	Article	IF	CITATIONS
109	Oxygen-Incorporated and Polyaniline-Intercalated 1T/2H Hybrid MoS2 Nanosheets Arrayed on Reduced Graphene Oxide for High-Performance Supercapacitors. Journal of Physical Chemistry C, 2018, 122, 8128-8136.	1.5	32
110	Nano-spatially confined and interface-controlled lithiation–delithiation in an <i>in situ</i> formed (SnS–SnS <sub>2</sub> –S)/FLG composite: a route to an ultrafast and cycle-stable anode for lithium-ion batteries. Journal of Materials Chemistry A, 2019, 7, 15320-15332.	5.2	32
111	Carbon nanomaterial-assisted morphological tuning for thermodynamic and kinetic destabilization in sodium alanates. Journal of Materials Chemistry A, 2013, 1, 5238.	5.2	30
112	Exfoliation of MoS <sub>2</sub> and h-BN nanosheets by hydrolysis of LiBH <sub>4</sub> . Nanotechnology, 2017, 28, 115604.	1.3	30
113	Phase tuning of P2/O3-type layered oxide cathode for sodium ion batteries via a simple Li/F co-doping route. Chemical Engineering Journal, 2022, 431, 134273.	6.6	30
114	Reversible hydrogen storage in yttrium aluminum hydride. Journal of Materials Chemistry A, 2017, 5, 6042-6046.	5.2	29
115	Citraconic anhydride as an electrolyte additive to improve the high temperature performance of LiNi0·6Co0·2Mn0·2O2/graphite pouch batteries. Journal of Alloys and Compounds, 2019, 805, 757-766.	2.8	29
116	A phosphorus and carbon composite containing nanocrystalline Sb as a stable and high-capacity anode for sodium ion batteries. Journal of Materials Chemistry A, 2020, 8, 443-452.	5.2	29
117	Scalable One-Pot Synthesis of Hierarchical Bi@C Bulk with Superior Lithium-Ion Storage Performances. ACS Applied Materials & Interfaces, 2020, 12, 51478-51487.	4.0	29
118	Introducing NO <sub>3</sub> <sup>–</sup> into Carbonateâ€Based Electrolytes via Covalent Organic Framework to Incubate Stable Interface for Liâ€Metal Batteries. Advanced Functional Materials, 2022, 32,	7.8	29
119	Fabrication of NiTi Shape Memory Alloys with Graded Porosity to Imitate Human Long-bone Structure. Journal of Bionic Engineering, 2015, 12, 575-582.	2.7	27
120	Controllable Hydrolysis Performance of MgLi Alloys and Their Hydrides. ChemPhysChem, 2019, 20, 1316-1324.	1.0	27
121	Influences of Composition on the Electrochemical Performance in Immiscible Snâ ``Al Thin Films as Anodes for Lithium Ion Batteries. Journal of Physical Chemistry C, 2009, 113, 18953-18961.	1.5	26
122	A synergistic strategy established by the combination of two H-enriched B–N based hydrides towards superior dehydrogenation. Journal of Materials Chemistry A, 2013, 1, 10155.	5.2	26
123	Nanosize-Controlled Reversibility for a Destabilizing Reaction in the LiBH <sub>4</sub> –NdH <sub>2+<i>x</i></sub> System. Journal of Physical Chemistry C, 2013, 117, 9566-9572.	1.5	26
124	Adding Metal Carbides to Suppress the Crystalline Li15Si4 Formation: A Route toward Cycling Durable Si-Based Anodes for Lithium-Ion Batteries. ACS Applied Materials & Interfaces, 2019, 11, 38727-38736.	4.0	26
125	Fluorine-substituted O3-type NaNi0.4Mn0.25Ti0.3Co0.05O2â^'F cathode with improved rate capability and cyclic stability for sodium-ion storage at high voltage. Journal of Energy Chemistry, 2021, 60, 341-350.	7.1	26
126	Realizing nano-confinement of magnesium for hydrogen storage using vapour transport deposition. Rare Metals, 2016, 35, 401-407.	3.6	25

#	Article	IF	CITATIONS
127	Dual arbon onfined SnS Nanostructure with High Capacity and Long Cycle Life for Lithiumâ€ion Batteries. Energy and Environmental Materials, 2021, 4, 562-568.	7.3	24
128	Applications of Plasma-Assisted Systems for Advanced Electrode Material Synthesis and Modification. ACS Applied Materials & Interfaces, 2021, 13, 13909-13919.	4.0	24
129	Microsized Sn supported by NiTi alloy as a high-performance film anode for Li-ion batteries. Journal of Materials Chemistry, 2012, 22, 9539.	6.7	23
130	Boosting Reversibility and Stability of Li Storage in SnO <sub>2</sub> –Mo Multilayers: Introduction of Interfacial Oxygen Redistribution. Advanced Materials, 2022, 34, e2106366.	11.1	23
131	Ammonia borane modified zirconium borohydride octaammoniate with enhanced dehydrogenation properties. Journal of Materials Chemistry A, 2015, 3, 5299-5304.	5.2	22
132	Effect of Pore Structure Regulation on the Properties of Porous TiNbZr Shape Memory Alloys for Biomedical Application. Journal of Materials Engineering and Performance, 2015, 24, 136-142.	1.2	22
133	The milled LiBH 4 / h- BN composites exhibiting unexpected hydrogen storage kinetics and reversibility. International Journal of Hydrogen Energy, 2017, 42, 15790-15798.	3.8	21
134	Microsized SnS/Few‣ayer Graphene Composite with Interconnected Nanosized Building Blocks for Superior Volumetric Lithium and Sodium Storage. Energy and Environmental Materials, 2021, 4, 229-238.	7.3	21
135	LiFâ€Induced Stable Solid Electrolyte Interphase for a Wide Temperature SnO <sub>2</sub> â€Based Anode Extensible to â^'50°C. Advanced Energy Materials, 2021, 11, 2101855.	10.2	20
136	Improved dehydrogenation of TiF <sub>3</sub> -doped NaAlH <sub>4</sub> using ordered mesoporous SiO <sub>2</sub> as a codopant. Journal of Materials Research, 2010, 25, 2047-2053.	1.2	19
137	Facile self-assembly of light metal borohydrides with controllable nanostructures. RSC Advances, 2014, 4, 983-986.	1.7	19
138	Enhanced cyclic stability of SnS microplates with conformal carbon coating derived from ethanol vapor deposition for sodium-ion batteries. Applied Surface Science, 2018, 436, 912-918.	3.1	19
139	Destabilizing the Dehydrogenation Thermodynamics of Magnesium Hydride by Utilizing the Immiscibility of Mn with Mg. Inorganic Chemistry, 2019, 58, 14600-14607.	1.9	19
140	Direct Detection and Visualization of the H <sup>+</sup> Reaction Process in a VO <sub>2</sub> Cathode for Aqueous Zinc-Ion Batteries. Journal of Physical Chemistry Letters, 2021, 12, 7076-7084.	2.1	19
141	Improved coulombic efficiency and cycleability of SnO <sub>2</sub> –Cu–graphite composite anode with dual scale embedding structure. RSC Advances, 2016, 6, 13384-13391.	1.7	17
142	Efficient Synthesis of Sodium Borohydride: Balancing Reducing Agents with Intrinsic Hydrogen Source in Hydrated Borax. ACS Sustainable Chemistry and Engineering, 2020, 8, 13449-13458.	3.2	17
143	Li2CO3 induced stable SEI formation: An efficient strategy to boost reversibility and cyclability of Li storage in SnO2 anodes. Science China Materials, 2021, 64, 2683-2696.	3.5	17
144	Structure and Deuterium Desorption from Ca <sub>3</sub> Mg <sub>2</sub> Ni <sub>13</sub> Deuteride: A Neutron Diffraction Study. Journal of Physical Chemistry C, 2014, 118, 4626-4633.	1.5	16

10

#	Article	IF	CITATIONS
145	Reaction Route Optimized LiBH <sub>4</sub> for High Reversible Capacity Hydrogen Storage by Tunable Surface-Modified AlN. ACS Applied Energy Materials, 2020, 3, 11964-11973.	2.5	16
146	Effective synthesis of magnesium borohydride via B-O to B-H bond conversion. Chemical Engineering Journal, 2022, 432, 134322.	6.6	16
147	H <sub>2</sub> Plasma Reducing Ni Nanoparticles for Superior Catalysis on Hydrogen Sorption of MgH <sub>2</sub> . ACS Applied Energy Materials, 2022, 5, 4976-4984.	2.5	16
148	Destabilization of LiBH <sub>4</sub> dehydrogenation through H <sup>+</sup> –H <sup>â^'</sup> interactions by cooperating with alkali metal hydroxides. RSC Advances, 2014, 4, 3082-3089.	1.7	15
149	Properties of WC–8Co hardmetals with plate-like WC grains prepared by plasma-assisted milling. Rare Metals, 2016, 35, 763-770.	3.6	15
150	Functional Materials Based on Metal Hydrides. Inorganics, 2018, 6, 91.	1.2	15
151	Ti <sub>3</sub> Sn–NiTi Syntactic Foams with Extremely High Specific Strength and Damping Capacity Fabricated by Pressure Melt Infiltration. ACS Applied Materials & Interfaces, 2019, 11, 28043-28051.	4.0	15
152	Ultralow Volume Change of P2â€Type Layered Oxide Cathode for Naâ€Ion Batteries with Controlled Phase Transition by Regulating Distribution of Na <sup>+</sup> . Angewandte Chemie, 2021, 133, 21128-21137.	1.6	15
153	Hydrogen generation properties and the hydrolysis mechanism of Zr(BH <sub>4</sub> ) <sub>4</sub> ·8NH <sub>3</sub> . Journal of Materials Chemistry A, 2017, 5, 16630-16635.	5.2	14
154	Achieving High Dehydrogenation Kinetics and Reversibility of LiBH <sub>4</sub> by Adding Nanoporous h-BN to Destabilize LiH. Journal of Physical Chemistry C, 2018, 122, 23336-23344.	1.5	14
155	Metalâ€Borohydrideâ€Modified Zr(BH <sub>4</sub> ) <sub>4</sub> â<8 NH <sub>3</sub> : Lowâ€Temperat Dehydrogenation Yielding Highly Pure Hydrogen. Chemistry - A European Journal, 2015, 21, 14931-14936.	ure 1.7	13
156	Flowerlike Ti-Doped MoO <sub>3</sub> Conductive Anode Fabricated by a Novel NiTi Dealloying Method: Greatly Enhanced Reversibility of the Conversion and Intercalation Reaction. ACS Applied Materials & Interfaces, 2020, 12, 8240-8248.	4.0	13
157	Synthesis of amorphous SeP2/C composite by plasma assisted ball milling for high-performance anode materials of lithium and sodium-ion batteries. Progress in Natural Science: Materials International, 2021, 31, 567-574.	1.8	13
158	Facile Synthesis of Peapodâ€Like Cu <sub>3</sub> Ge/Ge@C as a Highâ€Capacity and Longâ€Life Anode for Liâ€ Batteries. Chemistry - A European Journal, 2019, 25, 11486-11493.	on 1.7	12
159	Kinetically Controllable Hydrogen Generation at Low Temperatures by the Alcoholysis of CaMg <sub>2</sub> â€Based Materials in Tailored Solutions. ChemSusChem, 2020, 13, 2709-2718.	3.6	12
160	The Electrolyte Additive Effects on Commercialized Ni-Rich LiNi <sub><i>x</i></sub> Co <i><sub>y</sub></i> Mn <i>z</i> O <sub>2</sub> ( <i>x</i> + <i>y</i> + <i>z</i> ) Tj ET 2292-2299.	Qq0 0 0 r	gBT /Overlo
161	Construction of SnS-Mo-graphene nanosheets composite for highly reversible and stable lithium/sodium storage. Journal of Materials Science and Technology, 2022, 121, 190-198.	5.6	11

162Improving dehydrogenation properties of Mg/Nb composite films via tuning Nb distributions. Rare<br/>Metals, 2017, 36, 574-580.3.6

Мім Ζни

#	Article	IF	CITATIONS
163	Direct Rehydrogenation of LiBH4 from H-Deficient Li2B12H12â^'x. Crystals, 2018, 8, 131.	1.0	10
164	Improvement in the Electrochemical Lithium Storage Performance of MgH2. Inorganics, 2018, 6, 2.	1.2	9
165	Lithium–Sulfur Batteries: Self‧upported and Flexible Sulfur Cathode Enabled via Synergistic Confinement for Highâ€Energyâ€Density Lithium–Sulfur Batteries (Adv. Mater. 33/2019). Advanced Materials, 2019, 31, 1970236.	11.1	8
166	Direct Microstructural Evidence on the Catalyzing Mechanism for De/hydrogenation of Mg by Multi-valence NbOx. Journal of Physical Chemistry C, 2020, 124, 6571-6579.	1.5	7
167	Low temperature dehydrogenation properties of ammonia borane within carbon nanotube arrays: a synergistic effect of nanoconfinement and alane. RSC Advances, 2020, 10, 19027-19033.	1.7	7
168	In vitro and in vivo evaluation of porous NiTi alloy modified by sputtering a surface TiO2 film. Science China Technological Sciences, 2012, 55, 437-444.	2.0	6
169	Si-TiN alloy Li-ion battery negative electrode materials made by N2 gas milling. MRS Communications, 2018, 8, 1352-1357.	0.8	6
170	Breaking the Passivation: Sodium Borohydride Synthesis by Reacting Hydrated Borax with Aluminum. Chemistry - A European Journal, 2021, 27, 9087-9093.	1.7	6
171	A Nb-doped metal hydride electrode with overcharge resistance and wide temperature performance for aqueous rechargeable batteries. Scripta Materialia, 2022, 218, 114827.	2.6	6
172	Nanostructural Perspective for Destabilization of Mg Hydride Using the Immiscible Transition Metal Mn. Inorganic Chemistry, 2021, 60, 15024-15030.	1.9	5
173	Synthesis of NaBH <sub>4</sub> as a hydrogen carrier from hydrated borax using a Mg–Al alloy. Inorganic Chemistry Frontiers, 2022, 9, 370-378.	3.0	5
174	N-Doped Carbon Coated SnS/rGO Composite with Superior Cyclic Stability as Anode for Lithium-Ion Batteries. Industrial & Engineering Chemistry Research, 2022, 61, 4339-4347.	1.8	4
175	Achieving an H-induced transparent state in 200 nm thick Mg–Ti film by amorphization. Journal of Applied Physics, 2014, 115, 014304.	1.1	3
176	Na-Ion Batteries: A General Metal-Organic Framework (MOF)-Derived Selenidation Strategy for In Situ Carbon-Encapsulated Metal Selenides as High-Rate Anodes for Na-Ion Batteries (Adv. Funct. Mater.) Tj ETQq0 0 (	) r <b>gBT</b> /Ov	erl <b>a</b> ck 10 Tf 5
177	Reversible formation of metastable Sn-rich solid solution in SnO2-based anode for high-performance lithium storage. Applied Materials Today, 2021, 25, 101242.	2.3	3
178	Li–S Batteries: Unraveling the Catalytic Activity of Fe–Based Compounds toward Li <sub>2</sub> S <i><sub>x</sub></i> in Li–S Chemical System from <i>d</i> – <i>p</i> Bands (Adv.) Tj ETQ	q010002rgB	BT /Øverlock 1
179	Nanoconfined Oxidation Synthesis of Nâ€Doped Carbon Hollow Spheres and MnO 2 Encapsulated Sulfur Cathode for Superior Liâ€5 Batteries. Chemistry - A European Journal, 2018, 24, 4472-4472.	1.7	1
180	Li-lon Batteries: FeP@C Nanotube Arrays Grown on Carbon Fabric as a Low Potential and Freestanding	52	1

Anode for High-Performance Li-Ion Batteries (Small 30/2018). Small, 2018, 14, 1870138.

#	Article	IF	CITATIONS
181	A novel approach to the rapid in situ synthesis of WC nanopowder by plasma milling and carbothermal reduction. Advanced Engineering Materials, 0, , .	1.6	1
182	Batteries: Highly Stable Cycling of Amorphous Li <sub>2</sub> CO <sub>3</sub> -Coated α-Fe <sub>2</sub> O <sub>3</sub> Nanocrystallines Prepared via a New Mechanochemical Strategy for Li-Ion Batteries (Adv. Funct. Mater. 3/2017). Advanced Functional Materials, 2017, 27, .	7.8	0
183	Batteries: A New Strategy to Effectively Suppress the Initial Capacity Fading of Iron Oxides by Reacting with LiBH <sub>4</sub> (Adv. Funct. Mater. 16/2017). Advanced Functional Materials, 2017, 27, .	7.8	Ο
184	Innenrücktitelbild: Unveiling the Advances of Nanostructure Design for Alloyâ€Type Potassiumâ€Ion Battery Anodes via Inâ€Situ TEM (Angew. Chem. 34/2020). Angewandte Chemie, 2020, 132, 14801-14801.	1.6	0
185	Structure Analysis of FeSi <sub>2</sub> Embeded in Si by Transmission Electron Microscopy;. Materia Japan, 2001, 40, 1013-1013.	0.1	0